NUCL SCI TECH (2019) 30:72
https://doi.org/10.1007/s41365-019-0593-3

Dual-cavity beam arrival time monitor design for the Shanghai soft X-ray FEL facility

Shan-Shan Cao[1,2] · Ren-Xian Yuan[1] · Jian Chen[1,2] · Yong-Bin Leng[1]

Received: 30 May 2018 / Revised: 23 October 2018 / Accepted: 25 October 2018 / Published online: 9 April 2019

Abstract Free electron lasers provide high-power and ultrashort pulses with extreme brightness. In order to improve a facility's capabilities and explore the possibility of performing high-resolution time-resolved experiments, a beam arrival time resolution under 100 fs is required. In this article, a novel beam arrival time monitor (BAM) equipped with two cavities has been designed and a beam flight time measurement scheme based on the BAM prototype has been proposed to estimate phase jitter in the signal measurement system. The two BAM cavities work at different frequencies and the frequency difference is designed to be 35 MHz. Therefore, a self-mixing intermediate frequency signal can be generated using the two cavities. The measured beam flight time shows a temporal deviation of 37 fs (rms).

Keywords Beam arrival time monitor · Dual-cavities · Beam flight time · Self-mixing

This work was supported by the National Natural Science Foundation of China (No. 11575282).

✉ Yong-Bin Leng
lengyongbin@sinap.ac.cn

1 Shanghai Institute of Applied Physics, Chinese Academy of Sciences, Shanghai 201800, China

2 University of Chinese Academy of Sciences, Beijing 100049, China

1 Introduction

Free electron laser (FEL) has served as a useful and promising high-power and high-brightness light source in experimental studies (in the macroscopic world and at atomic and molecular levels), in static physical systems and ultrafast dynamic processes, and in investigations under simple experimental conditions to complex environments [1, 2]. The Shanghai soft X-ray FEL (SXFEL) was developed in phases. The test facility, named SXFEL test facility (SXFEL-TF), has been constructed in China at the Shanghai Synchrotron Radiation Facility (SSRF) campus and is presently under commissioning. It is a critical development step toward a hard X-ray facility [3, 4] and will be upgraded to the SXFEL user facility (SXFEL-UF) next year. The SXFEL-UF consists of two lines working on different FEL types. In particular, one of the beam lines will function as Self-Amplified Spontaneous Emission (SASE) self-seeding mode [5]. Table 1 shows the main beam parameters of the SXFEL.

The major challenge associated with such ultrashort, ultrafast, and high-brightness light pulses is the requirement of precise synchronization between the electron bunches and seed laser pulses in three-dimensional spaces [6–9]. This is because the seed FEL power relies on the energy exchange of electrons and photons along the undulator section. Energy exchange can only occur when the electron beam and seed laser are synchronized. Therefore, measuring the electron beam arrival time is a key issue for achieving synchronization in femtosecond resolution. Moreover, because SXFEL will be applied as a user facility, it is essential to exploit the possibility of time-resolved experiments, and such experiments demand high

Table 1 Main beam parameters of the SXFEL

Parameter	SXFEL-TF	SXFEL-UF
Electron energy (Gev)	0.84	1.5
Energy spread (rms)	$\leqslant$ 0.1%	$\leqslant$ 0.1%
Normalized emittance (mm mrad) (rms)	$\leqslant$ 2.0	$\leqslant$ 21.5
Bunch length (ps) (FWHM)	$\leqslant$ 1.0	$\leqslant$ 0.7
Bunch charge (nC)	0.5	0.5
Peak current at undulator (A)	$\leqslant$ 500	$\leqslant$ 700
Pulse repetition rate (Hz)	10	50

resolution of beam arrival time. In short, it is essential to conduct research on beam arrival time.

Currently, beam arrival time measurement is mainly based on the RF cavity scheme [10–13] and electro-optic sampling scheme [14, 15]. According to the published results, the best resolutions of the arrival time are 13 fs based on the RF cavity scheme and 6 fs [16] electro-optic detection scheme. Considering that the latter scheme requires greater cost and extreme complexity, the highly sensitive RF cavity based phase detection scheme was adopted. This scheme is realized with a specific metallic cavity. When an electron bunch passes through the cavity, the eigenmodes of an internal electromagnetic field of the cavity are excited owing to the wakefield effect [17, 18]. For a simple pillbox cavity, TM_{010} is radially symmetric and has the maximum value at its center. Its amplitude is proportional to the electron bunch charge and is independent of the beam offset [19].

There are various timing jitters that can influence the measurement of beam arrival time. The main jitter results from an electron beam timing jitter at various locations along the undulator. This is mainly because of the dispersive effects in the magnetic bunch compressor chicanes [20, 21]. The energy-dependent path leads to the conversion of a beam energy jitter to an arrival time jitter in the undulator. The energy jitter comes from the amplitude fluctuations and phase jitter of the accelerating fields, as well as the time jitter of the electron gun and reference clock. The typical detection scheme requires a highly stable reference signal that usually transmits over a long distance and is easily disturbed by temperature and humidity [22], etc. However, the SXFEL environment outside the tunnel currently is not suitable and the reference signal has larger jitter. In other words, this detection scheme applied at SXFEL may not attain appropriate results.

Therefore, a novel scheme using a dual-beam induced pickup signal mixing to measure the beam arrival time or beam flight time has been proposed. The proposed scheme is shown in Fig. 1. The beam arrival time monitor

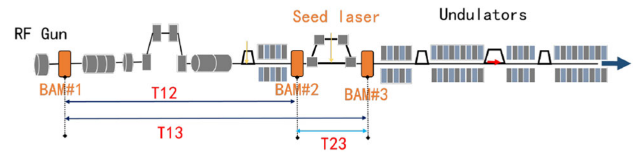

Fig. 1 (Color online) New proposed scheme to measure the beam arrival or beam flight time

(BAM)#1 is installed immediately behind the RF gun and its generated RF signal can be observed as the reference signal, because the time lag between the driven laser and RF signal is almost constant. Most importantly, this scheme is especially useful for the SASE self-seeding FEL because this facility focuses mainly on the beam flight time between the chicane's entrance and exit (T23). As the cavities are inside the tunnel where a stable environment exists, and have similar features (such as temperature sensitivity), this dual-cavities signal mixing scheme is expected to obtain better performance. In order to evaluate the practicability and performance of the new scheme, we designed a BAM equipped with two cavities working on different frequencies. In this research, we measured the beam flight times between BAM01's two cavities and between two BAMs. The layouts of the two BAMs are shown in Fig. 2.

The remainder of this paper is organized as follows. Section 2 introduces the basic principle of a BAM and presents the theoretical temporal resolution formula. In Sect. 3, the design process and simulation results are presented. Along with the simulated parameters, the theoretical temporal resolution is also calculated in this section. The cold test and beam flight time experiments based on the BAM prototypes are described in Sect. 4.

2 Basic principle of BAM

The BAM utilizes the high sensitivity and high resolution of a pillbox cavity to extract precise timing information. When a relativistic electron beam passes through a cavity, the beam interacts electromagnetically with its surroundings to generate an electromagnetic field, named the wakefield. The wakefield will cause energy loss from a beam to an electromagnetic field. The energy loss, E_{loss}, satisfies: [23]

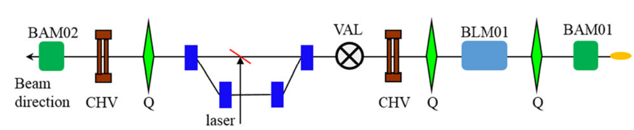

Fig. 2 (Color online) Layout of BAMs in SXFEL

$$E_{\text{loss}} = q^2 k_{\text{loss}} = q^2 \frac{[V(\mathbf{r})]^2}{4W}, \tag{1}$$

$$V(\mathbf{r}) = \int_0^L E(\mathbf{r}) e^{j\omega z/v}\,\mathrm{d}z \tag{2}$$

Here, q is the electron bunch charge, k_{loss} is the loss factor, L is the cavity length in the z direction, ω is the angular frequency, v is the velocity of the electron bunch, and W and E denote the stored energy and electric field intensity, respectively. Basically, the electromagnetic (EM) field inside the cavity is a superposition of several eigenmodes and the transverse field eigenmodes (TM) are combined with three indices: n(azimuthal), m(radial), and p(longitudinal). For TM_{010} mode, the longitudinal electric field ($E_{\mathrm{z},010}$) is:

$$E_{\mathrm{z},010}(r,t) = E_0 J_0\left(\frac{j_{01}}{a} r\right) e^{j\omega t}. \tag{3}$$

Here, J_0 is the 0-order Bessel function, j_{01} is the 1st root, and a is the cavity diameter. The output signal voltage of TM_{010} (V_{out}) can then be expressed as follows:

$$V_{\text{out}} = \frac{\omega q}{2}\sqrt{\frac{Z}{Q_{\text{ext}}}(R/Q)}\exp\left(-\frac{\omega^2\sigma_{\mathrm{z}}^2}{2c^2}\right). \tag{4}$$

Here Z is the characteristic impedance, which is designed to be 50 Ω usually, and σ_{z} is the electron bunch length. R / Q is the normalized shunt impedance. c is the light speed. Q_{ext} is the external quality factor that is determined by the cavity structure, especially the coupled structure; it is a constant for a given cavity, which complies with the following function:

$$\frac{1}{Q_{\mathrm{L}}} = \frac{1}{Q_0} + \frac{1}{Q_{\text{ext}}}. \tag{5}$$

Here, Q_{L} is the loaded quality factor; Q_0 is the internal quality factor; ideally it is determined by the material and structure of the cavity. It can be used to evaluate the cavity surface characteristic and energy storage. R / Q depends only on the cavity shape and is related to the beam offset. It describes the energy exchange between the cavity and electron bunches. If the electron beam passes the cavity in the z direction with an offset x and assuming $x \approx 0$, $E_{\mathrm{z}} =$ constant, the R / Q of TM_{010} can be calculated:

$$\frac{R}{Q} = \frac{2L\alpha_{\mathrm{T}}^2}{\omega\epsilon_0\pi J_1^2(j_{01})a^2}. \tag{6}$$

Here, α_{T} is the transit time factor. ϵ_0 is vacuum permittivity. J_1 is the 1-order Bessel function, j_{01} is its 1st root. It further shows that R / Q of a monopole is insensitive to the beam position near the cavity center. Thus, the output signal only depends on the electron bunch charge.

The above output signal voltage is a theoretical value. In fact, there are various noise components; one such component for the cavity is thermal noise. According to Nyquist's Theorem, thermal noise amplitude (V_{tn}) is represented as follows:

$$V_{\text{tn}} = \mathrm{NF}\cdot\sqrt{4k_{\mathrm{B}}TZ\Delta f}. \tag{7}$$

Here, k_{B} is the Boltzmann constant, T is the temperature, NF is the noise figure, Δf represents the bandwidth and can be expressed as follows: $\Delta f = f_{010}/Q_{\mathrm{L}}$, where f_{010} is the frequency of TM_{010}. Incidentally, a higher Q_{L} gives a narrower bandwidth for a determined frequency.

A more detailed discussion on the above theories can be found in Refs. [24–27]. A signal voltage in the time-domain (V_{total}) and frequency-domain ($F(w)$) as well as a detected phase (θ_{a}) can be expressed as follows:

$$V_{\text{total}}(t) = V_{\text{out}}(t) + V_{\text{tn}}(t). \tag{8}$$

$$F(w) = \int (V_{\text{out}}(t) + V_{\text{tn}}(t))e^{-iwt}\,\mathrm{d}t. \tag{9}$$

$$\begin{aligned}\theta_{\mathrm{a}} &= \arctan\frac{\mathrm{Re(F(w))}}{\mathrm{Im(F(w))}}\\ &= \arctan\frac{\mathrm{Re}(\mathrm{V_{out}(w)} + \mathrm{V_{tn}(w)})}{\mathrm{Im}(\mathrm{V_{out}(w)} + \mathrm{V_{tn}(w)})}\end{aligned} \tag{10}$$

Here Re and Im represent the real and imaginary parts, respectively. Therefore, the beam arrival time (T_{a}) can be described as follows:

$$T_{\mathrm{a}} = \frac{\theta_{\mathrm{a}}}{2\pi f_{010}}. \tag{11}$$

Hence, the time jitter caused by noises (t_{nj}) is as follows:

$$t_{\mathrm{nj}} = \frac{1}{2\pi f_{010}\cdot\mathrm{SNR}}. \tag{12}$$

Here, SNR is the ratio of signal to noise. In addition, another time shift resulting from frequency-error ($\Delta\omega$) due to the finite sampling time (t_{Qj}) is denoted as follows:

$$t_{\mathrm{Qj}} = \frac{\theta_0\Delta\omega}{\omega^2} = \frac{\pi}{\omega Q_{\mathrm{L}}^2}. \tag{13}$$

Considering the clock jitter (t_{cjitter}) from ADC sampling system and reference signal, the theoretical temporal resolution (Δt) can be derived as follows:

$$\Delta t = \sqrt{\left(\frac{1}{\omega_0\cdot\mathrm{SNR}}\right)^2 + \left(\frac{\pi}{\omega_0 Q_{\mathrm{L}}^2}\right)^2 + t_{\text{cjitter}}^2}. \tag{14}$$

3 Design and simulation results of BAM

3.1 Physical design of the BAM

A pillbox cavity is easier to fabricate as compared to a rectangular one. For this pillbox-like cavity, the highest excitation of all modes is the TM_{010} mode whose amplitude is proportional to the electron bunch charge only for a small beam offset [28]. The first dipole mode is the TM_{110} mode whose amplitude is proportional to the beam offset when it is close to the center. The second common mode is the TM_{020} mode which is similar than TM_{010} mode near the cavity center. Figure 3 shows the first four modes.

In this research, a dual-cavity BAM was designed whose pickups work at different resonance frequencies. The physical model is shown in Fig. 4. Each pickup has a pillbox cavity with two feedthroughs. This symmetrical design will not destroy the symmetry of the EM fields. Moreover, it is helpful in the beam tests, especially while conducting two or more measurements simultaneously. The cavity body is made of oxygen-free copper. Both ends of the BAM are connected to a 16 mm beam pipe. The two-dimensional section view of the BAM is presented in Fig. 5.

3.2 Simulation results

3.2.1 Frequency

Choosing an appropriate frequency is significant to the BAM. The resonant frequency of the TM_{010}-mode should be smaller than the cut-off frequency of the beam pipe to avoid their propagation into the beam pipe. For a circular waveguide, the cut-off frequency (f_c) of TE_{11}-mode can be calculated as follows:

$$f_c = \frac{1.841 \cdot c}{2\pi r_p}. \tag{15}$$

Here r_p is the beam pipe radius. Thus, the cut-off frequency of a TE_{11}-mode is 11 GHz for a circular waveguide with a 8-mm radius. Moreover, the choice of f_{010} should not be the integral or half-integral multiplication of an accelerating frequency of 2856 MHz to minimize the negative influence of dark current on measurement. Taking all factors into consideration, f_{010} of the dual-cavities are designed to be 4.685 GHz (cavity 1) and 4.72 GHz (cavity 2), respectively. The remainder of this section will focus on the cavity 1. For the specified cavity frequency, a cylindrical diameter is then determined. The cavity diameter (a) can be calculated as follows:

$$a = \frac{j_{01}}{\pi f_{010}\sqrt{\mu_0 \epsilon_0}}. \tag{16}$$

Here μ_0 and ϵ_0 are the permeability and permittivity of vacuum, respectively. For the cavity 1, a is 49 mm.

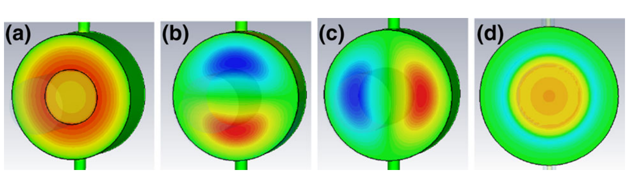

Fig. 3 (Color online) Excited modes in a cylindrical cavity: **a** TM_{010} mode, **b** TM_{110}–x mode, **c** TM_{110}–y mode, **d** TM_{020} mode

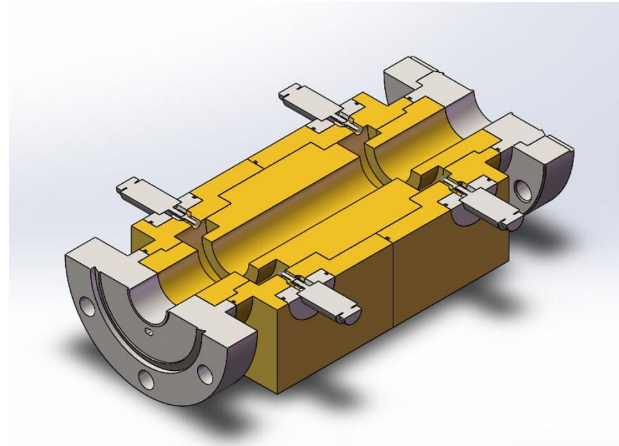

Fig. 4 (Color online) Physical model of the BAM

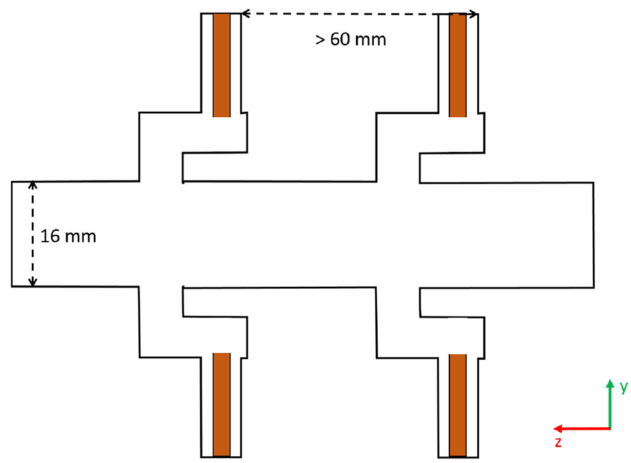

Fig. 5 Two-dimensional section view of the BAM

3.2.2 Cavity length

The cavity length has a great impact on the energy exchange between the electron beams and cavity. A narrow band cavity requires a high-quality factor Q_0 while a high Q_0 greatly depends on the cavity length. Based on the previous experience, a 1 MHz bandwidth can be obtained. Thus, Q_0 sets a lower limit on the cavity length L. For the monopole mode TM_{010} of a cylindrical cavity, the Q_0 can be calculated as follows:

$$Q_0 = \frac{2Lj_{01}^2}{2R_s\omega\epsilon_0(L + a/2)a}, \tag{17}$$

where R_s is the surface resistance. In addition, owing to the oscillating nature of the EM fields, the field inside the cavity will change when the electron bunch passes through the cavity. This phenomenon reduces the power coupling efficiency of the electron bunch into the cavity. Transit time factor α_T is used to characterize this factor, which is expressed as follows:

$$\alpha_T(\beta) = \text{sinc}\left(\frac{\omega L}{\beta c}\right), \tag{18}$$

where $\beta = v/c$. If the cavity is very long, transit time factor will reduce the power coupling efficiency. Thus, choosing a suitable cavity length is the trade-off between power coupling and quality factor (Q_0). As shown in Fig. 6 and Eqs. (17) (18), when the cavity length is $L = 6$ mm, Q_0 is about 5000, which enables the bandwidth to reach 1 MHz and α_T is larger than 0.8. Therefore, the cavity length is designed to be 6 mm.

3.2.3 Cavity structure and parameter

In this design, a re-entrant arrival time cavity is applied instead of an ordinary pillbox cavity. This structure offers convenience for frequency tuning during the manufacturing process. According to the theory of coaxial lines, the ratio of the inner and outer radius is preferably 2.3 to balance the output power and signal attenuation [29]. The probe diameter and insertion depth are set to be 1.5 mm and 0.25 mm, respectively. The cavity length can be adapted for each cavity radius to maintain the designed frequency. Moreover, as shown in Fig. 7, an external quality factor of 10^5 was appropriate to balance the voltage amplitude and TM_{010} mode bandwidth. When the external quality factor reaches 10^5, the bandwidth is almost constant, while the SNR keeps decreasing.

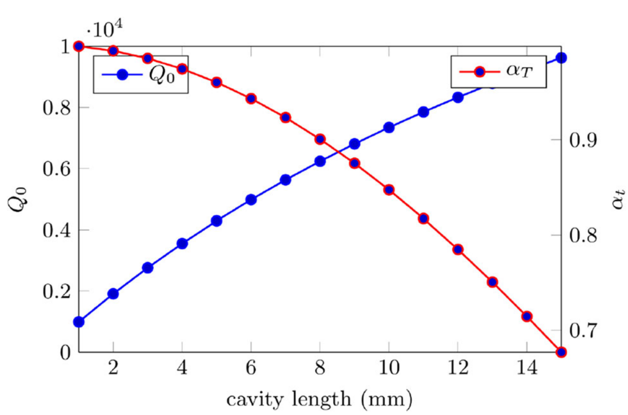

Fig. 6 (Color online) Correlations between quality factor (Q_0), transit factor (α_T), and cavity length

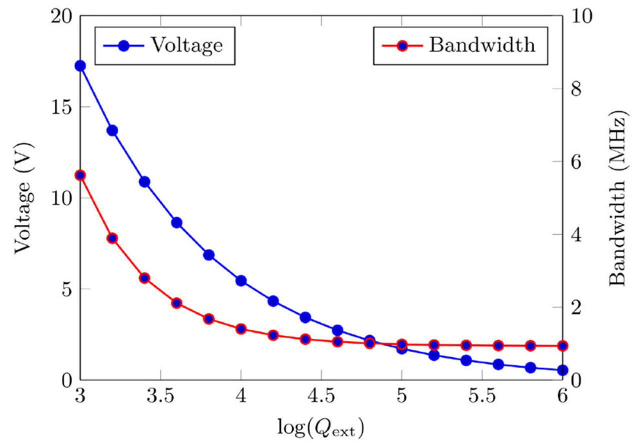

Fig. 7 (Color online) Correlations between output voltage (V_{out}), bandwidth (BW), and external quality factor (Q_{ext})

Furthermore, the cavity distance should be longer to avoid crosstalk between the two cavities. In this design, the distance is required to be larger than 60 mm; thus, the theoretical crosstalk is less than − 100 dB.

Once the cavity sizes were determined, their simulated parameters can further be calculated with the postprocessing template of the eigenmode solver, as displayed in Table 2. With the above-simulated results and Eq. (14), the theoretical temporal resolution is approximately 3.5 fs when the SNR was assumed to be 80 dB.

4 The BAM test results

4.1 Cold test

To validate the RF-characteristic of the BAM, two sets of BAM prototypes have been fabricated and tested with a network analyzer in the laboratory.

Table 2 Simulated parameters of the BAM

Parameters	Value (Cavity 1)	Value (Cavity 2)
Frequency (GHz)	4.685	4.72
Q_0	4796	4835
Q_{ext} ($\times 10^5$)	1.8	1.9
Q_{load}	4671	4716
R / Q (Ω)	107.2	107.9
τ[a] (ns)	317.7	318
Bandwidth (MHz)	1.00	1.02

[a]Decay time constant

Table 3 displays the cold test results of BAM01 and BAM02. It can be seen that the measured frequencies are 4.6852 GHz and 4.7204 GHz for BAM01, and 4.729 GHz and 4.685 GHz for BAM02. The 3 dB bandwidths are 1.1109 MHz and 1.0578 MHz for BAM01, and 1.24 MHz and 1.16 MHz for BAM02. In short, the cold test results agree well with the simulation results, which implies that the prototype can meet the demands of the beam experiments.

4.2 Beam flight time experiments

The two BAMs have been installed in the injector section of the SXFEL test facility and the distance between the two BAMs is approximately 40 m. A beam flight time detection experiment based on the new proposed scheme (the dual-cavities signals mixing scheme) can be performed. This experiment consists of two parts: the beam flight time between BAM01's two cavities, the beam flight time between BAM01-A and BAM02-A cavities. As discussed above, the first experiment is mainly used to evaluate the performance of the measurement system. The second part is actually used to measure the two BAMs' beam flight times. Figure 8 shows the beam flight time detection setup based on the dual-cavities signals mixing scheme. The system consists of four parts: a BAM capturing the beam induced RF signal, an RF front-end, a signal acquisition processor, and an online/offline signal processing system.

The raw RF signals from two BAMs' four cavities were captured by an oscilloscope with a sampling rate of 20 GHz. Figure 9 shows the four RF signal in time-domain and frequency-domain. In particular, BAM01-B and BAM02-A signals are used as the local oscillator (LO) signals. As the LO input is an exponentially damped sinusoidal signal, the dynamic range and linearity of the mixer will deteriorate with the attenuation of the LO signal.

Currently, the whole signal processing electronics system is placed outside the tunnel for convenient operation in this preliminary research. Thus, low noise and phase-stable cables are required for the RF front-end realized analog down conversions, bandpass filtering, and amplification of RF signals.

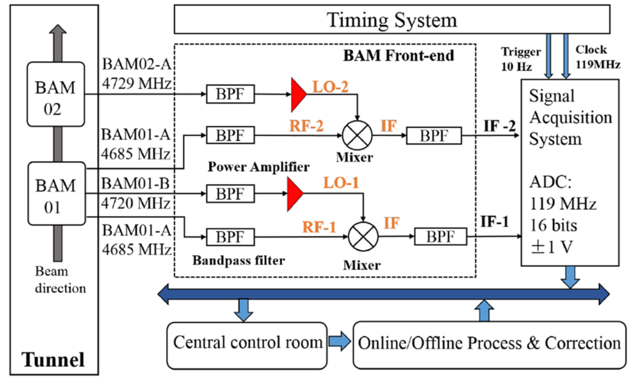

Fig. 8 Beam flight time detection setup based on dual-cavities signals mixing scheme

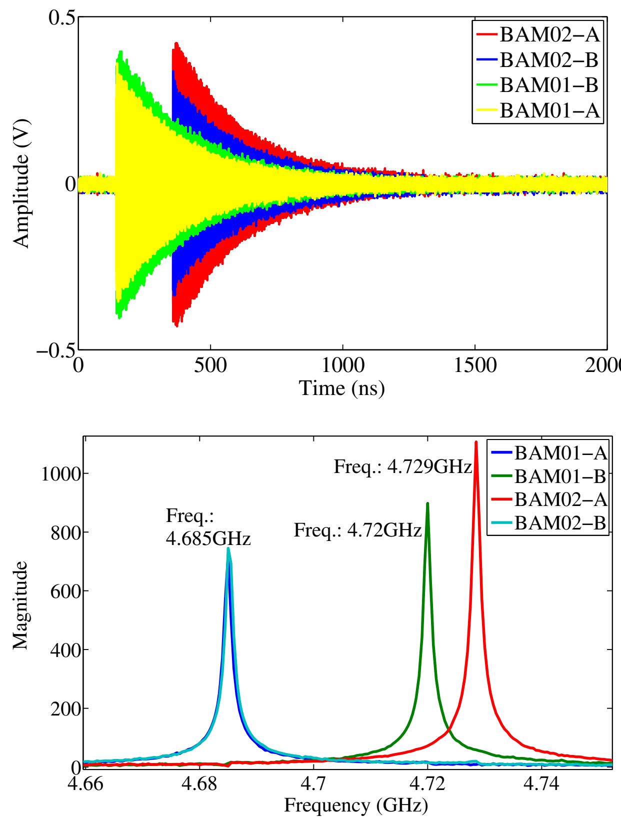

Fig. 9 (Color online) Time-domain signals and frequency spectra of the four output signals from BAM01 and BAM02

Table 3 Cold test results

Parameters	BAM01-A	BAM01-B	BAM02-A	BAM02-B
Frequency (GHz)	4.6852	4.7204	4.729	4.685
Frequency difference (MHz)	0.2	0.4	9	0
Bandwidth (MHz)	1.11	1.06	1.24	1.16
Bandwidth difference (MHz)	0.108	0.035	0.215	0.158

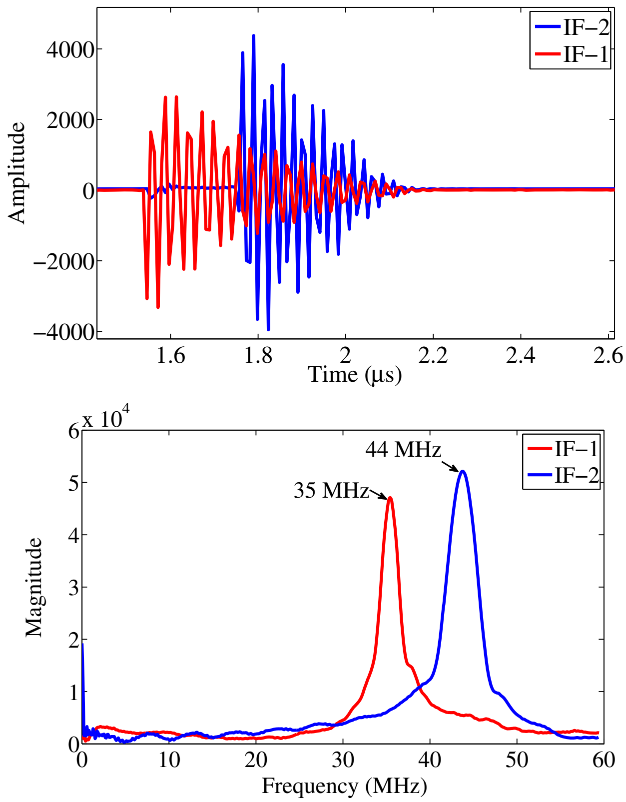

Fig. 10 (Color online) Two generated IF signals output waveforms and their frequency spectra

After self-mixing, the two generated intermediate frequency (IF) signals are shown in Fig. 10. Their peak amplitudes are approximately 0.2 h, which is considerably smaller than the full scale of the analog–digital converter (ADC), i.e., 1 h. The frequencies of IF-1 and IF-2 are 35 MHz and 44 MHz, respectively. IF-1 is the measured beam flight time between BAM01's two cavities, while IF-2 represents the beam flight time between BAM01 and BAM02.

The IF signals are then digitized by a 16-bit ADC with a sampling rate of 119 MHz. This signal acquisition processor works at an external trigger of (10 Hz) and external clock mode of (119 MHz). The obtained digital IF signal is processed and corrected online or offline.

The measured two beam flight times over 40 min are given in Fig. 11. The deviations of IF-1 and IF-2 are 37 fs and 51 fs, respectively. For the beam flight times between BAM01's two cavities, the limitation mainly comes from the unoptimized electronics and environmental noise. For the beam flight time between the two BAMs, the beam jitter is additionally a jitter source apart from the measurement system limitations.

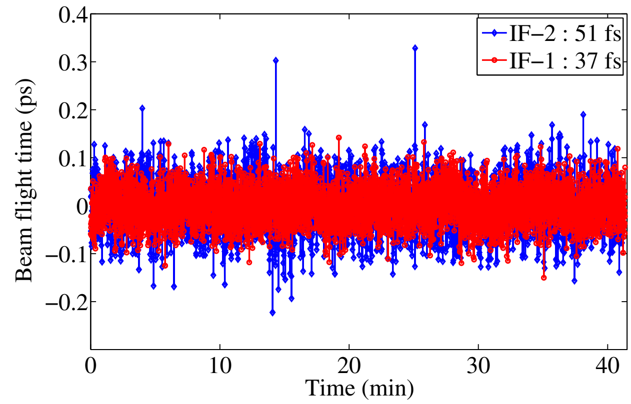

Fig. 11 (Color online) Two beam flight time deviations

5 Summary

To measure the beam arrival time with the limitations of a poor reference signal, a dual-cavities signals mixing scheme is proposed and it is especially useful for the SASE self-seeding FEL facility that focuses more on the beam flight time. Based on this, a BAM equipped with two cavities working at 4.685 GHz and 4.72 GHz, respectively, is designed and two sets of BAMs were installed at the SXFEL injector section. Moreover, two beam flight time experiments, one between a single BAM's two cavities, and the other between the two BAMs have been investigated to evaluate the performance of the measurement system and the practicability of the new proposed scheme. The measured beam flight times show a standard deviation of 37 fs and 51 fs, respectively, and they are significantly larger than the theoretical values. This is mainly due to the unoptimized electronics and environmental noise, etc. Therefore, further investigations are ongoing, such as planting the whole system inside the tunnel, optimizing the RF front-end system. Moreover, further experiments will be conducted soon to demonstrate how close the real system values may become to these promising theoretical values.

Acknowledgements The authors thank the operation team of SXFEL for its assistance in conducting the beam experiment.

References

1. C. Feng, D.Z. Huang, H.X. Deng et al., A single stage EEHG at SXFEL for narrow-bandwidth soft X-ray generation. Sci. Bull. **61**, 1202–1212 (2016). https://doi.org/10.1007/s11434-016-1140-9
2. C. Feng, H.X. Deng, Review of fully coherent free-electron lasers. Nucl. Sci. Tech. **29**, 160 (2018). https://doi.org/10.1007/s41365-018-0490-1
3. Z.T. Zhao, S.Y. Chen, L.H. Yu et al., Shanghai soft X-ray free electron laser test facility. in *Proceedings of 2nd International*

Particle Accelerator Conference. (San Sebastián, Spain, 2011), pp. 3011–3013

4. Z.T. Zhao, C. Feng, K.Q. Zhang et al., Two-stage EEHG for coherent hard X-ray generation based on a superconducting linac. Nucl. Sci. Tech. **28**, 117 (2017). https://doi.org/10.1007/s41365-017-0258-z
5. Z.T. Zhao, D. Wang, Q. Gu et al., SXFEL: A soft X-ray free electron laser in China. Synchrotron Radiat. News **30**, 29–33 (2017). https://doi.org/10.1080/08940886.2017.1386997
6. P. Craievich, S.D. Mitri, A.A. Zholents, Single-bunch emittance preservation in the presence of trajectory jitter for FERMI elettra-seeded FEL. Nucl. Instrum. Methods A **604**, 457–465 (2009). https://doi.org/10.1016/j.nima.2009.03.106
7. L.H. Yu, Generation of intense UV radiation by subharmonically seeded single-pass free-electron lasers. Phys. Rev. A **44**, 5178 (1991). https://doi.org/10.1103/PhysRevA.44.5178
8. R. Bonifacio, C. Pellegrini, L.M. Narducci, Collective instabilities and high-gain regime in a free electron laser. Opt. Commun. **50**, 373–378 (1984). https://doi.org/10.1016/0030-4018(84)90105-6
9. A.M. Kondratenko, E.L. Saldinet, Generating of coherent radiation by a relativistic electron beam in an ondulator. Part. Accel. **10**, 207–216 (1980)
10. M. Hansli, B. Zeitler, A. Angelovski et al., A beam arrival time cavity for regae at desy. in *Proceedings of 5th International Particle Accelerator Conference*. (Dresden, Germany, 2014), pp. 1820–1822. https://doi.org/10.18429/JACoW-IPAC2014-TUPRI104
11. T. Ohshima, H. Maesaka, Y. Otake et al., Variation of beam arrival timing at SACLA. in *Proceedings of 34th Free Electron Laser Conference*. (Nara, Japan, 2012), pp. 317–320
12. J. Hong, C. Kim, J.H. Han et al., Bunch arrival time monitor for PAL-XFEL. in *Proceedings of 3rd International Beam Instrumentation Conference*. (Monterey, CA, USA, 2014), pp. 191–194
13. A. Brachmann, C. Bostedt, J. Bozek et al., Bunch arrival time monitor for PAL-XFEL. in *Proceedings of 1st International Particle Accelerator Conference*. (Kyoto, Japan, 2010), pp. 2287–2289
14. V. Arsov, M. Felber, E. A.Knabbe et al., Electro-optic bunch arrival time measurement at FLASH. in *Proceedings of 11th European Particle Accelerator Conference*. (Genoa, Italy, 2008), pp. 3348–3350
15. Y. Otake, Advanced diagnosis of the temporal characteristics of ultra-short electron beams. Nucl. Instrum. Methods A **637**, S7–S11 (2011). https://doi.org/10.1016/j.nima.2010.02.010
16. F. Löhl, V. Arsov, M. Felber et al., Electron bunch timing with femtosecond precision in a superconducting free-electron laser. Phys. Rev. Lett. **104**, 144801 (2010). https://doi.org/10.1103/PhysRevLett.104.144801
17. R. Lorenz, Cavity beam position monitors. AIP. Conf. Proc. **451**, 53 (2008). https://doi.org/10.1063/1.57039
18. A.W. Chao, *Physics of Collective Beam Instabilities in High Energy Accelerators*, 1st edn. (Wiley, New York, 1993), p. 371
19. Y. Inoue, H. Hayano, Y. Honda et al., Development of a high-resolution cavity-beam position monitor. Phys. Rev. ST Accel. Beams **11**, 062801 (2008). https://doi.org/10.1103/PhysRevSTAB.11.062801
20. Z. Zhou, W.H. Huang, Y.C. Du et al., Beam compression dynamics and associated measurement methods in superconducting THz source. in *Proceedings of 6th International Particle Accelerator Conference*. (Richmond, VA, USA, 2015), pp. 969–971. https://doi.org/10.18429/JACoW-IPAC2015-MOPTY015
21. P. Craievich, S.D. Mitri, M. Milloch et al., Modeling and experimental study to identify arrival-time jitter sources in the presence of a magnetic chicane. Phys. Rev. ST Accel. Beams **16**, 090401 (2013). https://doi.org/10.1103/PhysRevSTAB.16.090401
22. M. Liu, X.L. Dai, C.X. Yin et al., Preliminary design of a femtosecond timing system for large accelerator facilities. Nucl. Sci. Tech. **29**, 32 (2018). https://doi.org/10.1007/s41365-018-0369-1
23. Q. Luo, B.G. Sun, D.H. He, Design of s-band re-entrant cavity BPM. Nucl. Sci. Tech. **20**, 133 (2009). https://doi.org/10.13538/j.1001-8042/nst.20.133-139
24. N.Y. Joshi, Design and analysis techniques for cavity beam position monitor systems for electron accelerators. Dissertation, University of London (2013)
25. T. Nakamura, Development of beam-position monitors with high position resolution. Dissertation, University of Tokyo (2008)
26. V. Sargsyan, Cavity Beam Position Monitor for the TESLA-cryomodule. Cross-Talk minimization. Dissertation, Technical University of Berlin (2003)
27. J. Chen, Y.B. Leng, L.Y. Yu et al., Beam test results of high Q CBPM prototype for SXFEL. Nucl. Sci. Tech. **28**, 51 (2017). https://doi.org/10.1007/s41365-017-0195-x
28. C. Simon, S. Chel, P. Contrepois et al., Beam position monitors using a reentrant cavity. in *Proceeding of the 8th European Workshop on Beam Diagnostic and Instrumentation for Particle Accelerator*. (Venice, Italy, 2007), pp. 93–95
29. N. Marcuvitz, Waveguide Handbook (Electromagnetics and Radar). (1986). https://doi.org/10.1049/PBEW021E